

Cell Reports Medicine, Volume 5

Supplemental information

**PD-L1-expressing tumor-associated macrophages
are immunostimulatory and associate with good
clinical outcome in human breast cancer**

Lei Wang, Weihua Guo, Zhikun Guo, Jiangnan Yu, Jiayi Tan, Diana L. Simons, Ke Hu, Xinyu Liu, Qian Zhou, Yizi Zheng, Egelston A. Colt, John Yim, James Waisman, and Peter P. Lee

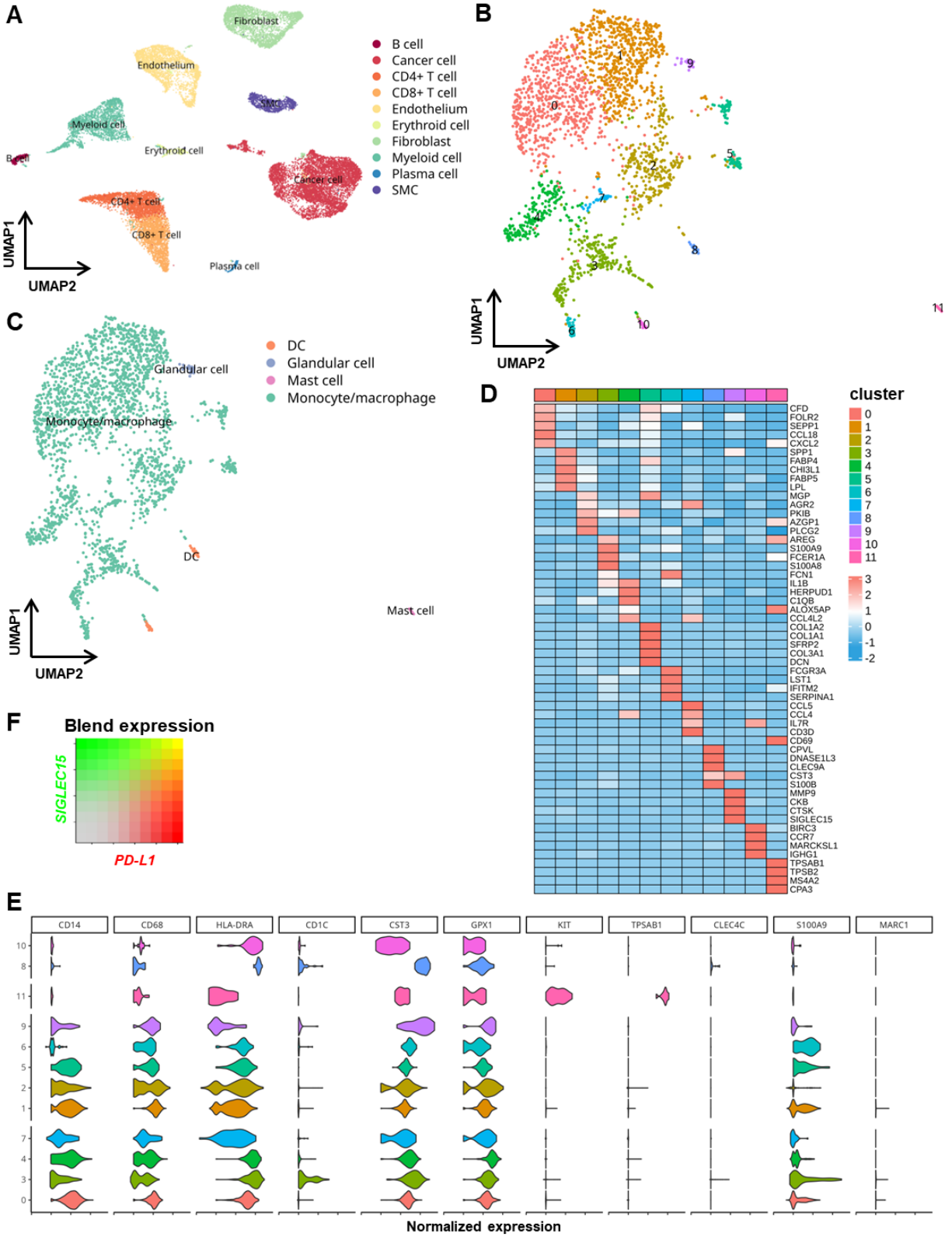


Figure S1. Single-cell analysis with blended expression analysis of PD-L1 and SIGLEC15 identified the PD-L1^{+hi} and PD-L1^{-lo} monocytes/macrophages, related to Figure 1. (A) 10 major cell types were identified and annotated in TME. **(B)** 12 clusters were identified in myeloid cells with the optimal clustering resolution ($r = 0.5$). **(C)** Monocytes/macrophages were identified and annotated in TME. **(D)** Average expression heatmap of the top 5 markers of each cluster. **(E)** Violin plot of the expression of key myeloid cell markers crossing all the myeloid cell clusters. **(F)** Blend expression of *PD-L1* and *SIGLEC15* on monocytes/macrophages.

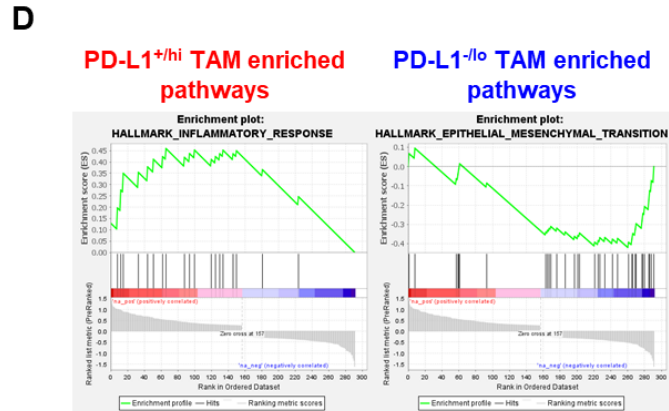
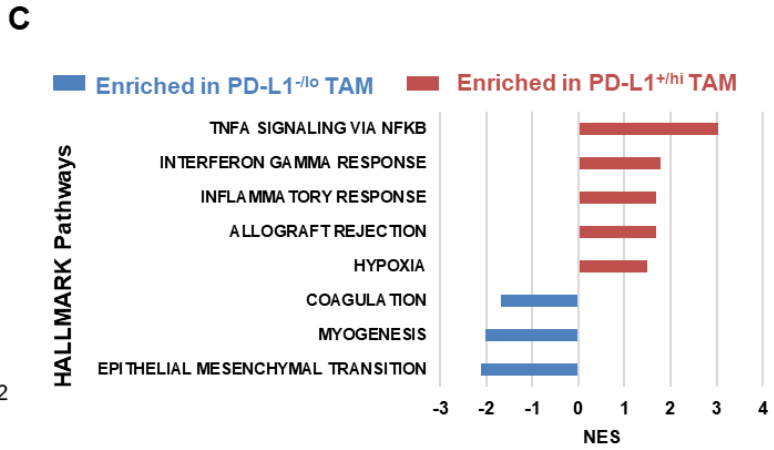
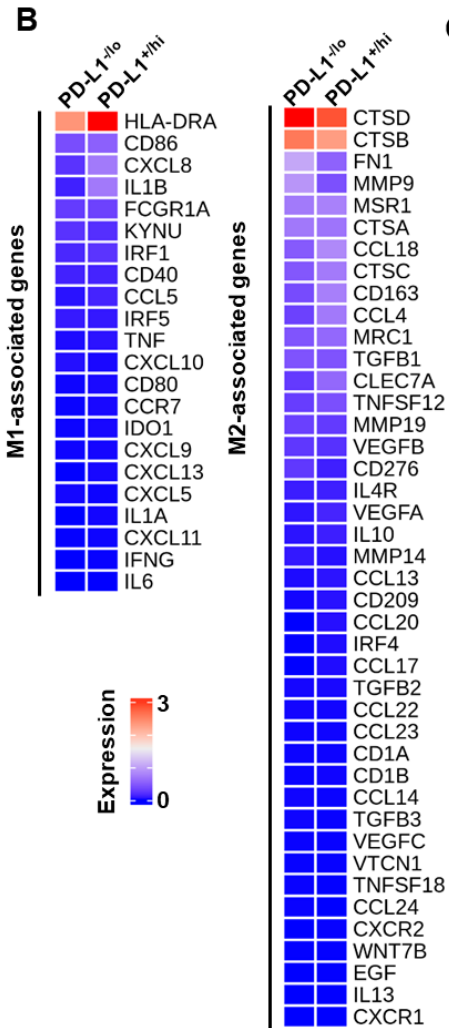
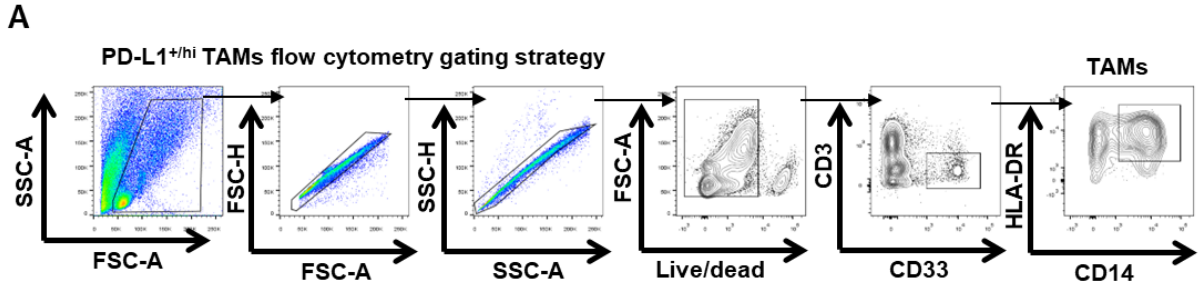


Figure S2. PD-L1^{+/hi} and PD-L1^{-/lo} TAMs dichotomy confirmed by flow cytometry, related to

Figure 1. (A) Representative flow plots showing the gating of TAMs from human breast tumor.

(B) Expression levels of M1- or M2-associated genes in PD-L1⁺ and PD-L1⁻ TAMs. **(C)** All

significantly enriched pathways from gene-set enrichment analysis of PD-L1⁺ and PD-L1⁻ TAMs based on the differential expressed genes (DEGs) identified by scRNA-seq (FDR q-value<0.1).

(D) Enrichment plot of representative enriched pathways for PD-L1⁺ and PD-L1⁻TAMs.

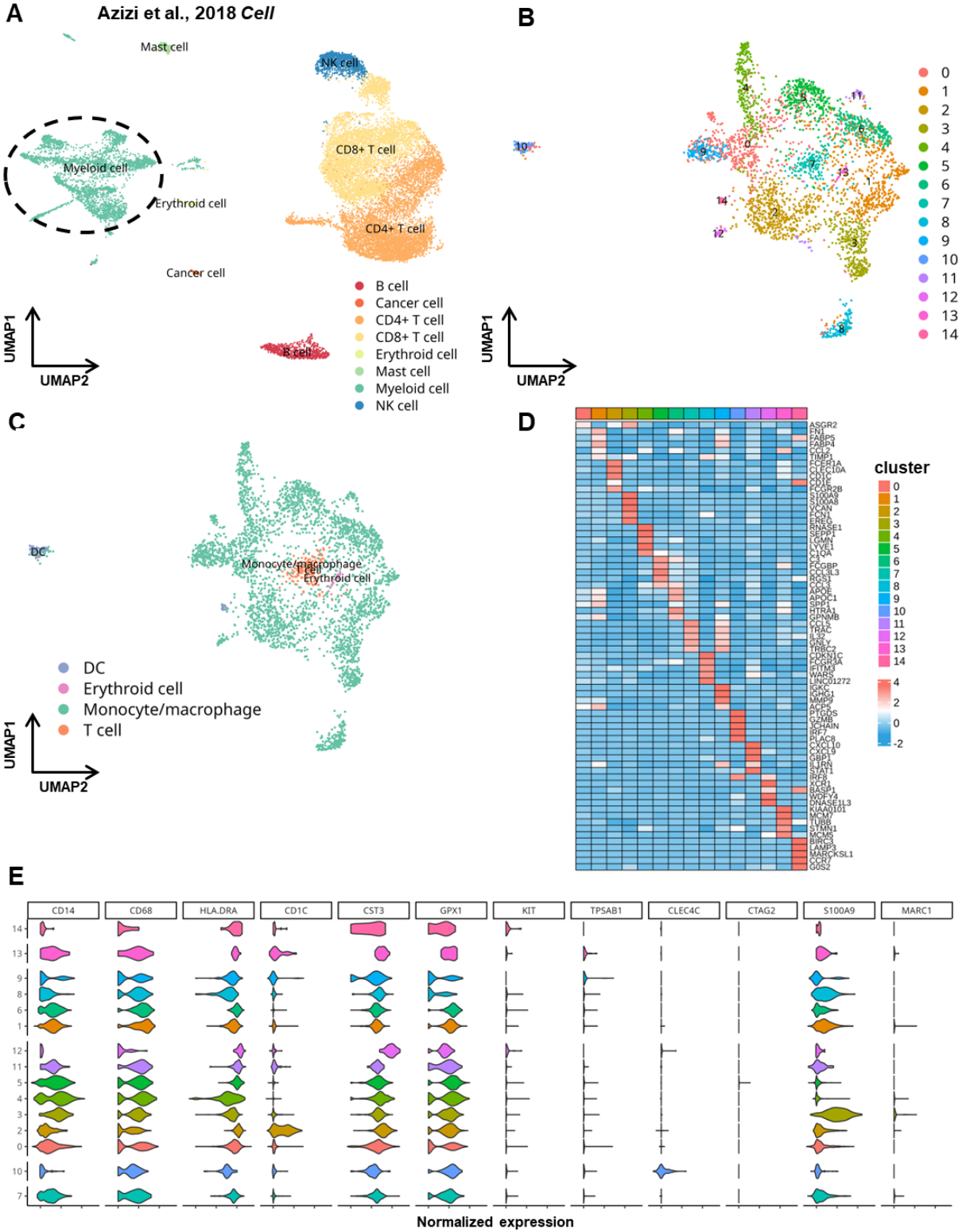
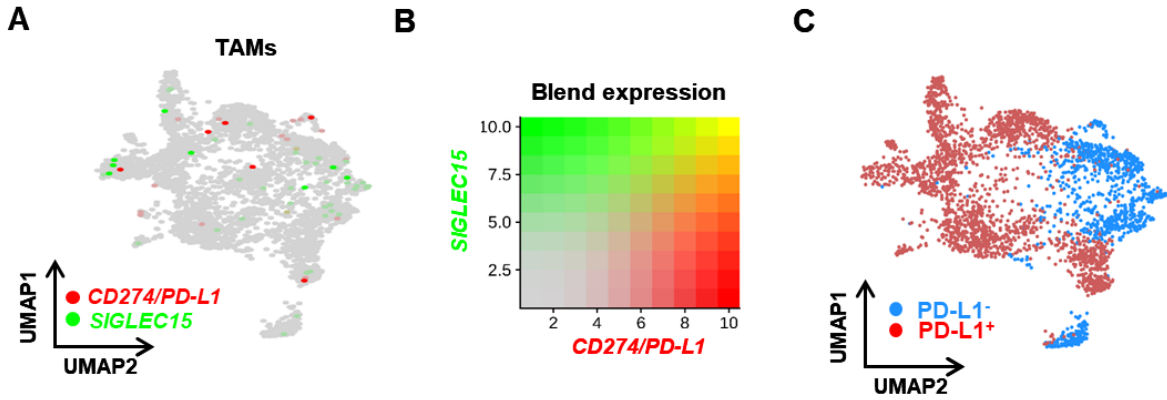
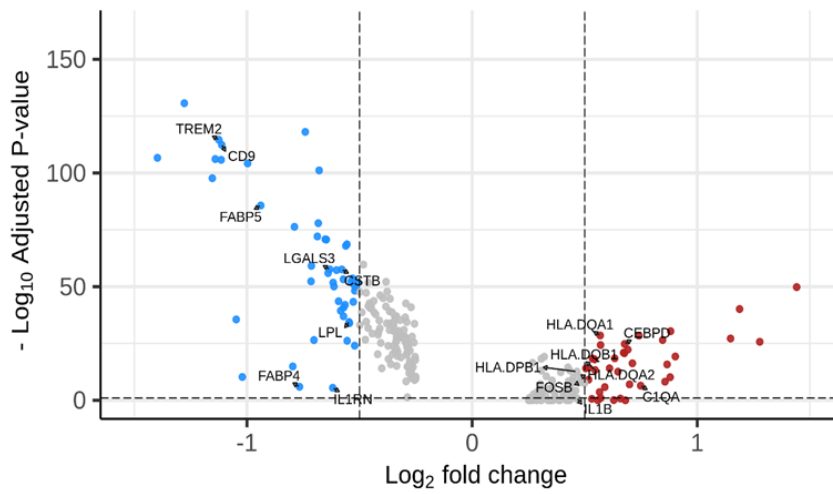


Figure S3. Single-cell analysis identified the PD-L1^{+hi} and PD-L1^{-lo} monocytes/macrophages (Azizi et al., *Cell* 2018), related to Figure 1. (A) 8 major cell types were identified and annotated in TME. (B) 15 clusters were identified in myeloid cells with the optimal clustering resolution ($r = 0.6$). (C) Monocytes/macrophages were identified and annotated in TME. (D) Average expression heatmap of the top 5 markers of each cluster. (E) Violin plot of the expression of key myeloid cell markers crossing all the myeloid cell clusters.



D ● Upregulated in *PD-L1*^{-/lo} TAMs ● Upregulated in *PD-L1*^{+/hi} TAMs



E

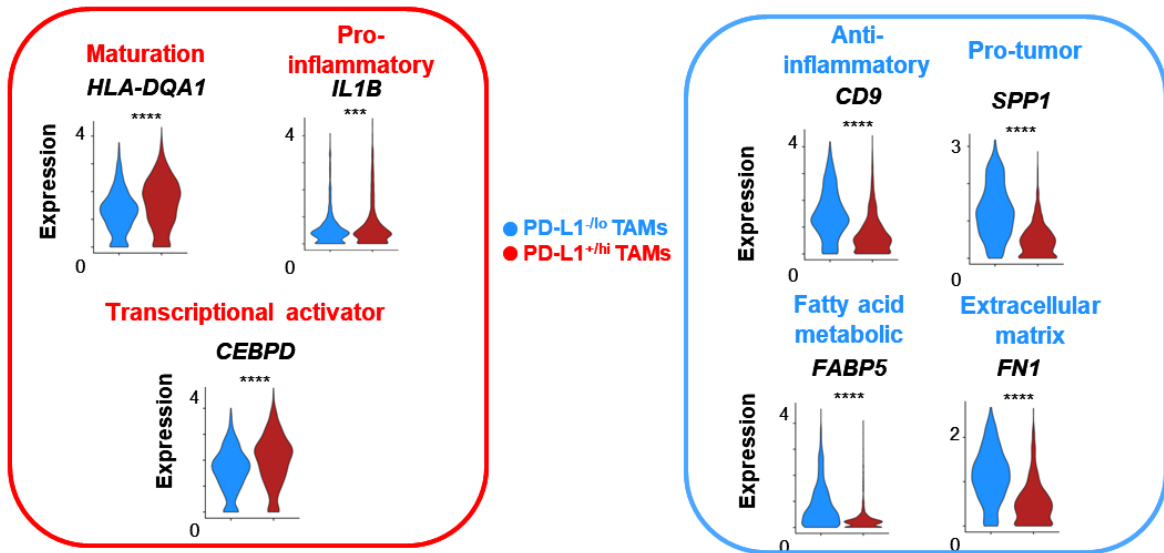


Figure S4. Expression profile differences between PD-L1⁺ and PD-L1⁻ TAMs validated in public scRNA-seq data (Azizi et al., *Cell* 2018), related to Figure 1. (A) UMAP of TAMs (*CD14⁺CD68⁺HLA-DR⁺*, n=3,130 cells) from the public scRNA-seq data. (B) Blend expression of *PD-L1* and *SIGLEC15*. (C) The dichotomization of the TAM clusters into *PD-L1⁺/SIGLEC15⁻* and *PD-L1⁻/SIGLEC15⁺* subpopulations. (D) Volcano plot showing differentially expressed genes (DEGs) between the subpopulation of PD-L1⁺ or PD-L1⁻ TAMs. (E) Expression distribution of selected genes involved in maturation, pro-inflammatory or transcriptional activator and anti-inflammatory, pro-tumor, fatty acid metabolic or extracellular matrix between PD-L1^{+hi} and PD-L1^{-lo} TAMs.

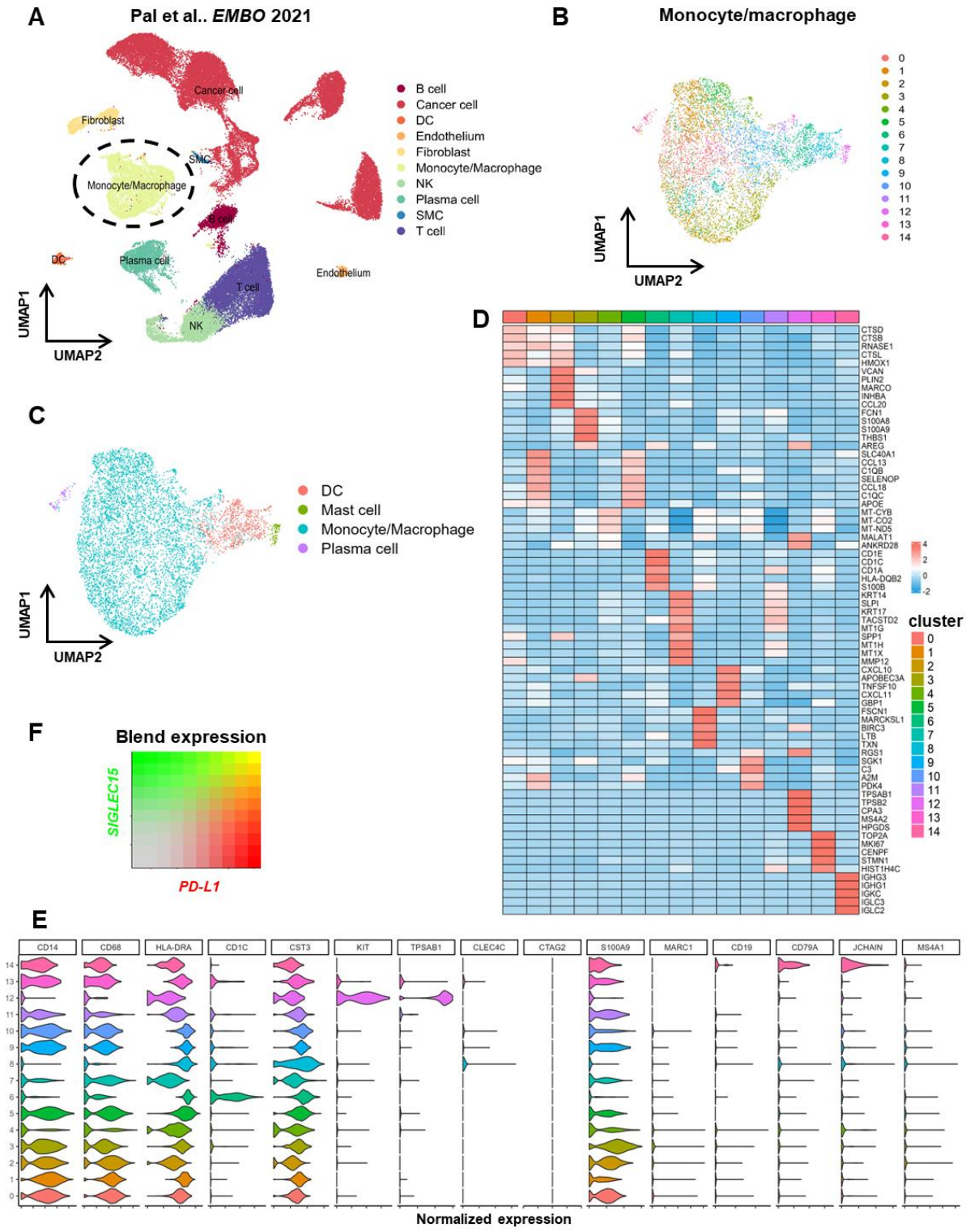


Figure S5. Single-cell analysis identified the PD-L1^{+hi} and PD-L1^{-lo} monocytes/macrophages (Pal et al., *EMBO* 2021), related to Figure 2. (A) 10 major cell types were identified and annotated in TME. (B) 15 clusters were identified in myeloid cells with the optimal clustering resolution ($r = 0.8$). (C) Monocytes/macrophages were identified and annotated in TME. (D) Average expression heatmap of the top 5 markers of each cluster. (E) Violin plot of the expression of key myeloid cell markers crossing all the myeloid cell clusters. (F) Blend expression of *PD-L1* and *SIGLEC15* on monocytes/macrophages.

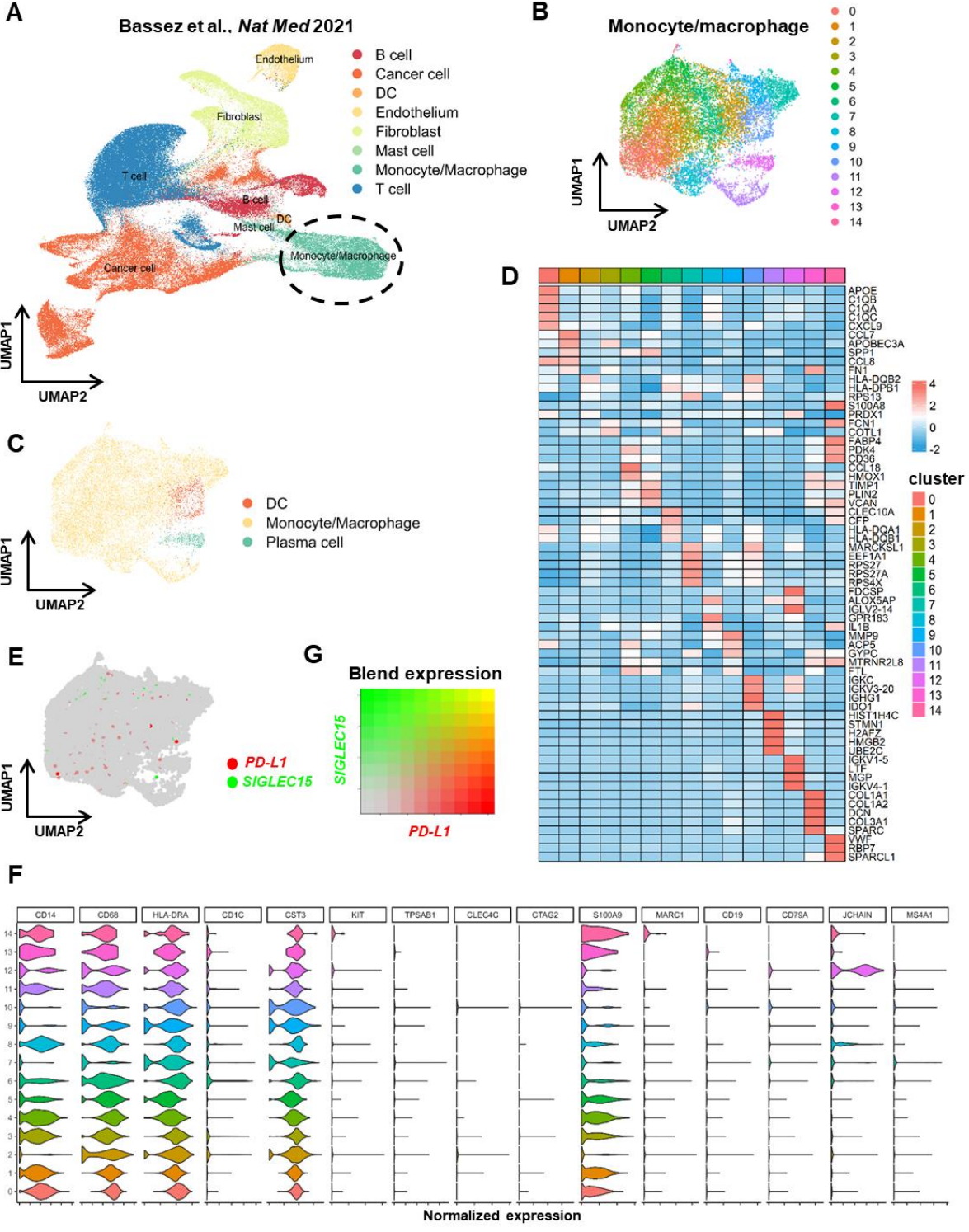


Figure S6. Single-cell analysis identified the PD-L1^{+hi} and PD-L1^{-lo} monocytes/macrophages (Bassez et al., *Nat Med* 2021), related to Figure 2. (A) 8 major cell types were identified and annotated in TME. (B) 15 clusters were identified in myeloid cells with the optimal clustering resolution ($r = 0.8$). (C) Monocytes/macrophages were identified and annotated in TME. (D) Average expression heatmap of the top 5 markers of each cluster. (E) Mutually exclusive expression of *PD-L1* and *SIGLEC15* in myeloid cells. (F) Violin plot of the expression of key myeloid cell markers crossing all the myeloid cell clusters. (G) Blend expression of *PD-L1* and *SIGLEC15* on monocytes/macrophages.

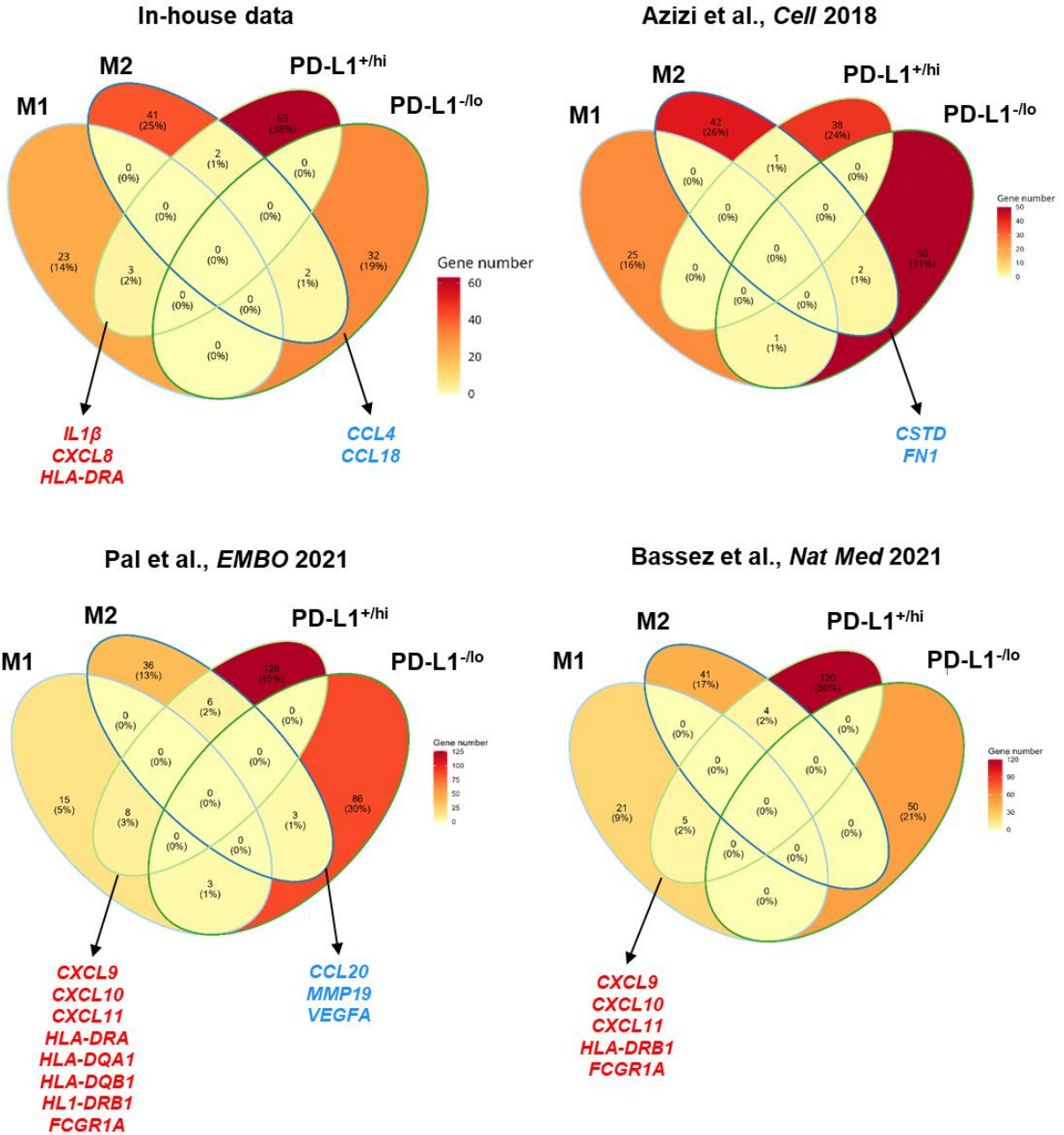


Figure S7. Venn diagram analysis of the overlap genes between PD-L1^{+hi} or PD-L1^{-lo} DEGs with M1 or M2 marker genes using in-house and public scRNA-seq data, related to Figure 3.

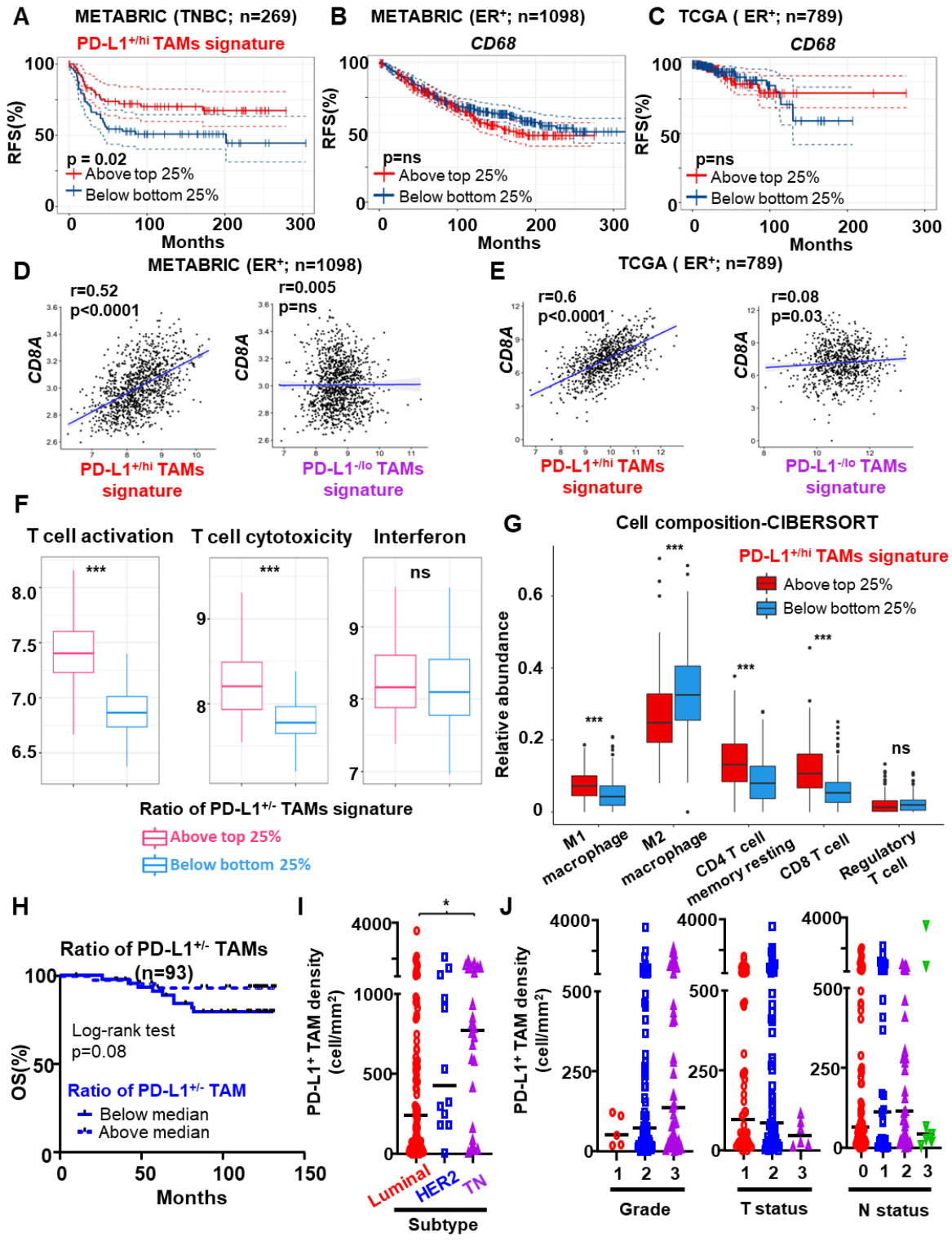
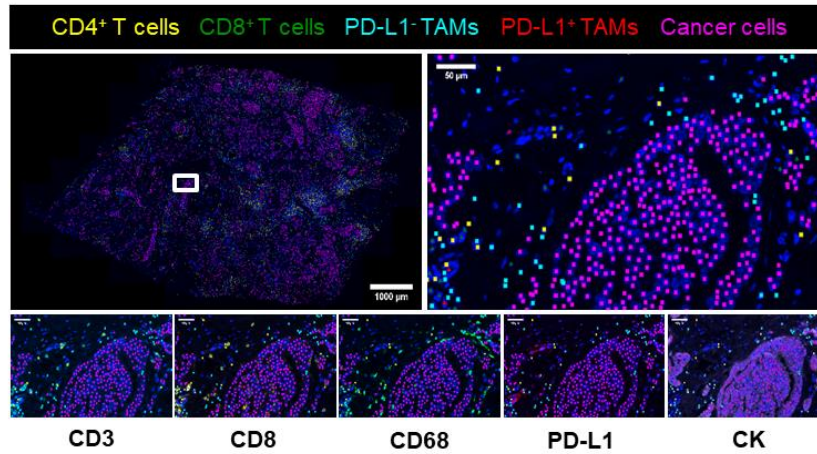
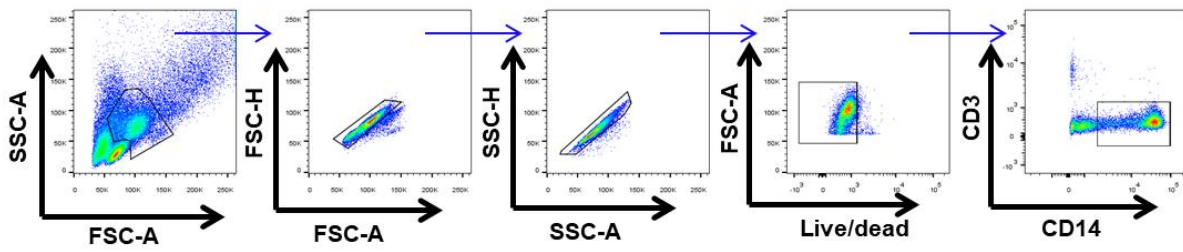


Figure S8. Analysis of PD-L1⁺ and PD-L1⁻ TAMs gene signature in public bulk-tumor transcriptomic datasets, related to Figure 3. (A) Kaplan-Meier relapse-free survival (RFS) curves and log-rank test generated for the gene signature of PD-L1^{+hi} TAMs⁻ in the TNBC cohort of METABRIC (n=269) dataset. (B-C) Kaplan-Meier RFS curves and log-rank test generated for the gene expression of *CD68* in the luminal BC cohorts of METABRIC (n=1098) (B) and TCGA (n=789) (C) datasets. (D-E) The association between *CD8A* expression and PD-L1⁺ or PD-L1⁻ TAMs gene signature in METABRIC (D) and TCGA (E) datasets. Correlation coefficient test. (F) Gene signatures of T cell activation, T cell cytotoxicity or interferon were compared between patients with high vs. low gene signature ratio of PD-L1⁺/PD-L1⁻ TAMs in the luminal BC cohort of METABRIC (n=1098). (G) Cell composition differences determined by CIBERSORT deconvolution method between tumors with high- and low-expressing gene signature of PD-L1^{+hi} TAMs. Patients were divided into high- and low-expressing groups based on a 25% cut-off of the gene signature or *CD68* expression. ****p<0.0001. (H) Kaplan-Meier overall survival (OS) curves and log-rank test generated for above or below median density ratio of PD-L1⁺/PD-L1⁻ TAMs in cohort #2 (n=93). (I) The density of PD-L1⁺ TAMs in BC patients with luminal, HER2 or TN subtype (n=129). (J) The density of PD-L1⁺ TAMs in combined cohort #1 and 2 (n=142) with various tumor grade, T status and N status. *p<0.05.

A**B****CD14⁺ monocyte flow gating strategy****C***In vitro* differentiation

3 days

Monocytes $\xrightarrow{\text{Human serum (5%)}}$ Macrophages

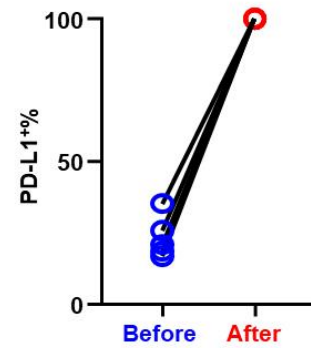
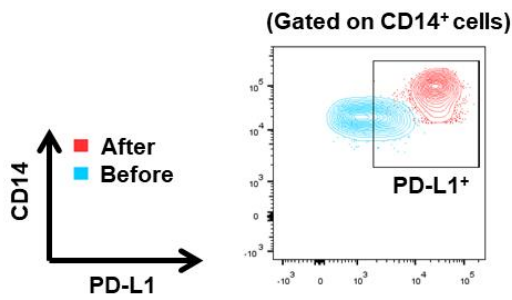
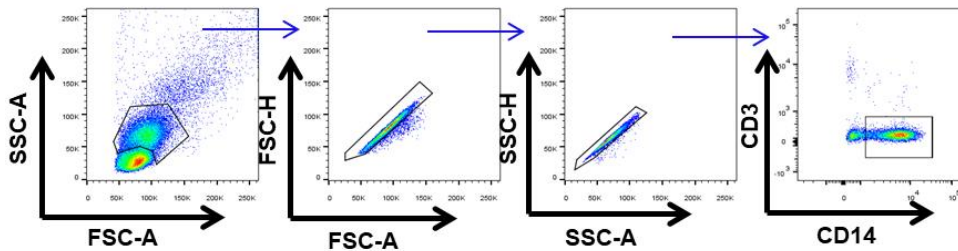
**D****CD14⁺ monocyte phosflow gating strategy**

Figure S9. PD-L1 is upregulated during the monocyte-macrophage differentiation, related to Figure 5. (A) Representative multiple immunofluorescence staining of breast tumor tissue section for PD-L1⁺ TAMs (CD68⁺PD-L1⁺), PD-L1⁻ TAMs (CD68⁺PD-L1⁻), CD8⁺ T cells (CD8⁺), CD4⁺ T cells (CD3⁺CD8⁻) and cancer cells (CK⁺). (B) Representative flow plots showing the gating strategy of peripheral blood monocytes from patients with BC. (C) Schematic and the representative flow plot of PD-L1 expression after in vitro macrophage differentiation. (D) Representative flow plots showing the gating strategy of peripheral monocytes in phosflow cytometry.

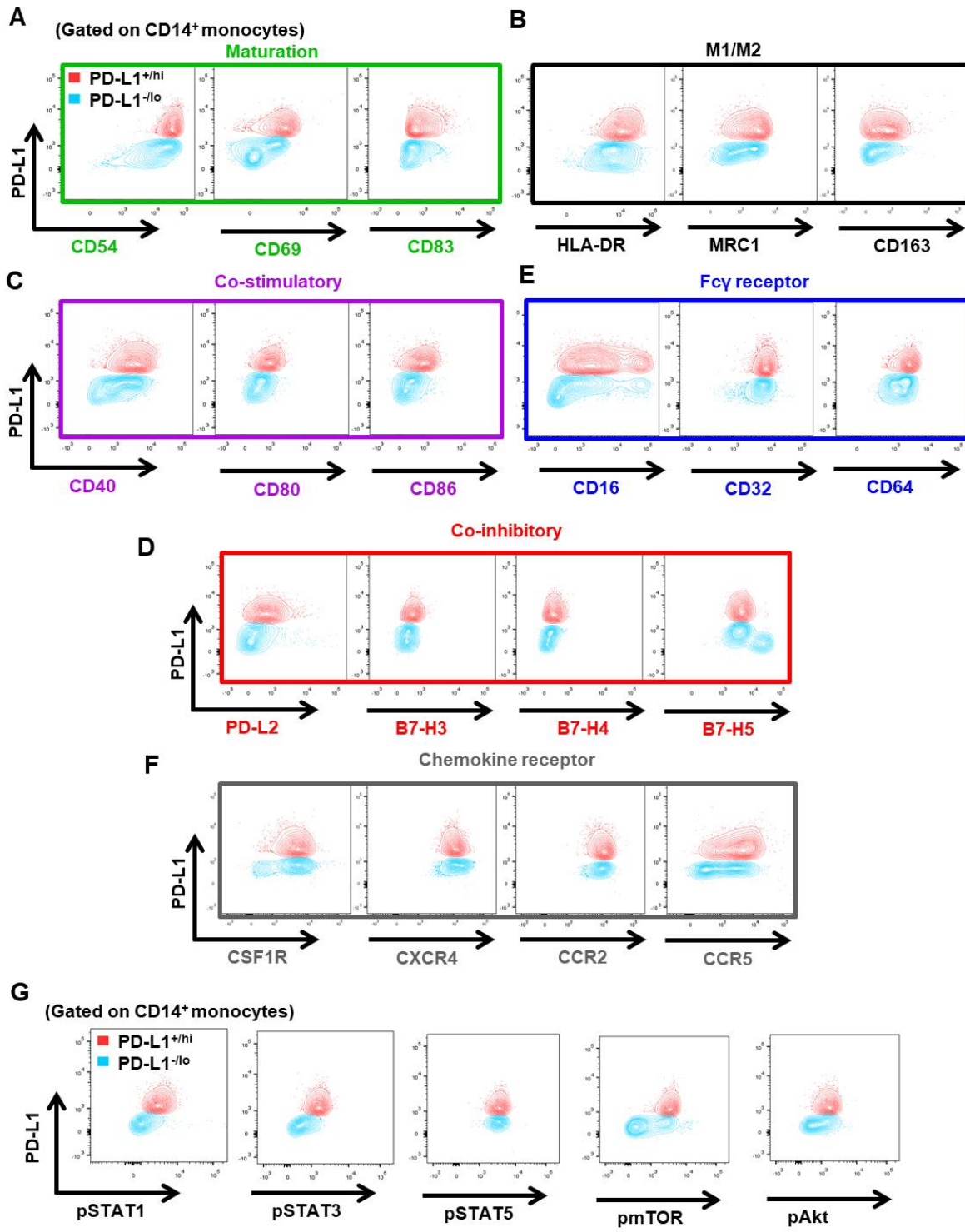


Figure S10. Protein expression profiles of PD-L1⁺ and PD-L1⁻ monocytes, related to Figure 5. (A-F) Representative flow plots showing the expression of surface proteins of maturation (A), M1/M2 marker (B), co-stimulatory ligands (C), co-inhibitory ligands (D), Fcγ receptors (E) and chemokine receptors (F). (G) Representative flow plots showing the levels of phosphorylated signal transduction proteins.

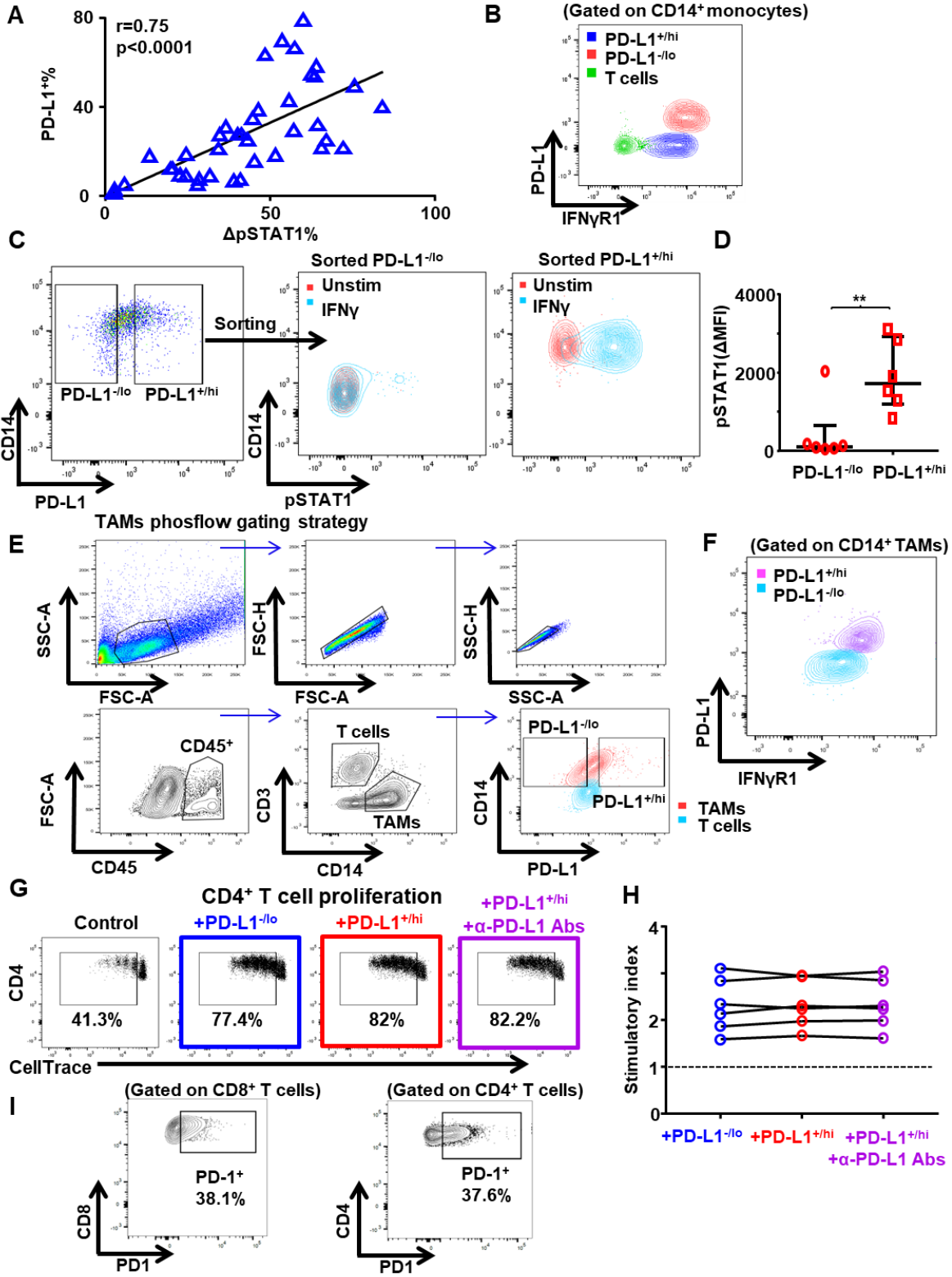


Figure S11. PD-L1⁺ TAMs are primed for IFN γ stimulation, related to Figure 6. (A) The association between PD-L1⁺% and IFN γ -induced STAT1 phosphorylation (Δ pSTAT1%) in peripheral monocytes from patients with BC (n=40). Pearson's correlation coefficient test. (B) Representative flow plots showing the levels of IFN γ R1 in PD-L1⁺ and PD-L1⁻ monocytes. (C-D) IFN γ -induced STAT1 phosphorylation were shown in representative flow plots (C) and were compared between flow sorted PD-L1^{+hi} and PD-L1^{-lo} peripheral monocytes (D). **p<0.01. Paired t test. (E) Representative flow plots showing the gating strategy of TAMs from breast tumors in phosflow cytometry. (F) Representative flow plots showing the levels of IFN γ R1 in PD-L1⁺ and PD-L1⁻ TAMs. (G-H) CellTrace Violet dilution by CD4⁺ T cells determined after 4 days of TCR-stimulated coculture with autologous PD-L1⁺ or PD-L1⁻ monocytes/macrophages from patients with BC at a 1 to 1 ratio (n=6). (G) Representative flow plots showing percentage of proliferated CD8⁺ T cells. (H) The proliferation stimulation activity was measured by the cell number ratio of (CD8/CD4+CD14)/(CD8/CD4) as the stimulatory index. (I) Representative flow plots showing the expression of PD1 on CD8⁺ and CD4⁺ T cells during the CellTrace proliferation assays.

Table S1. M1 vs. M2 gene signature, related to Figure 1 and 3.

M1	M2
<i>FCGR1A</i>	<i>MRC1</i>
<i>CD40</i>	<i>CD163</i>
<i>CD80</i>	<i>CD209</i>
<i>CD86</i>	<i>CD1A</i>
<i>HLA-DRA</i>	<i>CD1B</i>
<i>HLA-DRB1</i>	<i>CXCR1</i>
<i>HLA-DQA1</i>	<i>CXCR2</i>
<i>HLA-DQB1</i>	<i>IL4R</i>
<i>IRF1</i>	<i>EGF</i>
<i>IRF5</i>	<i>CTSA</i>
<i>IDO1</i>	<i>CTSB</i>
<i>KYNU</i>	<i>CTSC</i>
<i>CCR7</i>	<i>CTSD</i>
<i>IFNG</i>	<i>CLEC7A</i>
<i>TNF</i>	<i>WNT7B</i>
<i>IL1A</i>	<i>FASLG</i>
<i>IL1B</i>	<i>TNFSF12</i>
<i>IL6</i>	<i>TNFSF18</i>
<i>CXCL8</i>	<i>CD276</i>
<i>IL12B</i>	<i>VTCN1</i>
<i>IL23A</i>	<i>MSR1</i>
<i>CXCL9</i>	<i>FN1</i>
<i>CXCL10</i>	<i>IRF4</i>
<i>CXCL11</i>	<i>VEGFA</i>
<i>CXCL13</i>	<i>VEGFB</i>
<i>CCL5</i>	<i>VEGFC</i>
	<i>VEGFD</i>
	<i>TGFB1</i>
	<i>TGFB2</i>
	<i>TGFB3</i>
	<i>MMP9</i>
	<i>MMP14</i>
	<i>MMP19</i>
	<i>IL4</i>
	<i>IL10</i>
	<i>IL13</i>
	<i>CCL4</i>
	<i>CCL13</i>
	<i>CCL14</i>
	<i>CCL17</i>
	<i>CCL18</i>
	<i>CCL20</i>
	<i>CCL22</i>
	<i>CCL23</i>
	<i>CCL24</i>

Table S2. Gene signature of PD-L1^{+/−}TAMs generated from scRNA-seq, related to Figure 3.

PD-L1 ⁺ TAM			PD-L1 [−] TAM		
Gene	Log ₂ FC	Related-function	Gene	Log ₂ FC	Related-function
<i>IL1B</i>	1.40	Pro-inflammatory	<i>SPP1</i>	-1.61	Pro-tumor
<i>HLA-DQA1</i>	1.12	Maturation	<i>FABP5</i>	-1.06	Metabolism
<i>HLA-DPB1</i>	1.10	Maturation	<i>FN1</i>	-0.75	ECM organization
<i>CEBPD</i>	1.06	Activation	<i>IL1RN</i>	-0.71	Anti-inflammatory
<i>FCER1A</i>	1.02	Pro-inflammatory	<i>CSTB</i>	-0.68	Anti-inflammatory
<i>SEPP1</i>	0.99	Anti-tumor	<i>LDHA</i>	-0.51	Metabolism
<i>HLA-DQB1</i>	0.94	Maturation			
<i>FOSB</i>	0.81	Activation			

**Note: The METABRIC analysis used expression levels of the gene signature;
The TCGA analysis used expression levels of the gene signature normalized to *CD68*.**

Table S3. The characteristics of patients with luminal breast cancer, related to Figure 3.

	Cohort #1 Whole-slide	Cohort #2 TMA
Characteristics	N=49 (%)	N=93 (%)
Age—yr		
Median	51	55
Range	27-93	29-87
Tumor stage— no.(%)		
DCIS	1 (2)	0 (0)
T1	20 (41)	34 (37)
T2	23 (47)	58 (62)
T3	5 (10)	1 (1)
Grade— no.(%)		
G1	5 (10)	0 (0)
G2	28 (57)	68 (73)
G3	16 (33)	25 (27)
Nodal status— no.(%)		
N0	25 (51)	48 (52)
N1-3	22 (45)	45 (48)
Unknown	2 (4)	0 (0)